ANALYSIS OF AC-DRIVEN ELECTROOSMOTIC FLOW IN A MICROCHANNEL PACKED WITH MICROSPHERES

Y.J. Kang, C. Yang* and X.Y. Huang

School of Mechanical and Production Engineering
Nanyang Technological University, Singapore 639798, mcyang@ntu.edu. sg

ABSTRACT

This paper presents an analysis of the alternating current (AC) electroosmotic flow in open- and closed-end cylindrical microchanneles packed with microspheres. The time-periodic electroosmotic flow in an open capillary in response to the application of an AC electric field is obtained using the Green's function approach. The analysis is based on the capillary model. The backpressure associated with the counter-flow in a closed capillary is solved using the Brinkman's momentum equation. The results obtained from this study can be used for the development of novel electrokinetic microactuators.

Keywords: ac electroosmosis, porous media, closed channel, microchannel flow, green's function method

1 INTRODUCTION

Electroosmosis (EO) mostly is associated with a DC (direct current) electric field, which is used to generate a steady-state electroosmotic flow (EOF). A similar effect occurs with an AC (alternating current) electric field. In this situation, however, the electroosmotic flow becomes time and frequency dependent. Recently, the AC electroosmosis has drawn a wide attention by researchers [1-2].

With examination of the current literature known to the authors, no study on the AC electroosmotic flow in porous media has yet been reported. However, use of porous structures can enhance the pressure-building capacity of the AC electroosmotic flow. Paul *et al.* [3] proposed a method to generate high pressure using DC electroosmosis through a microchannel packed with microparticles. The pressure of 10 atm at 1.5 kV applied voltage have been achieved using fused-silica capillaries packed with charged 1.5 μm silica beads. In a recent work by Zeng *et al.* [4], an EO pump was fabricated to generate maximum pressures in excess of 20 atm or maximum flow rates of 3.6 μl/min for a 2 kV applied DC potential. Recently, a new separation mode for capillary electrochromatography using AC was proposed by Nakagawa *et al.* [5] as an application to control the chemical retention of a sample solute.

This paper presents an analysis of the AC electroosmotic flow in a cylindrical microcapillary packed with microspheres of uniform size. Two different conditions regarding the channel ends are considered. When the channel is open, i.e., both ends are connected to the reservoirs, the oscillating EOF is analyzed using the capillary flow model. The corresponding Navier-Stokes equation is solved using Green's function method and the complete Poisson-Boltzmann equation governing the electric double layer (*EDL*) potential field is solved with arbitrary zeta potentials under an analytical scheme. When both the capillary ends are closed, the oscillating flow generated by the AC electroosmosis is balanced by the counter-flow. The associated backpressure is solved using the Brinkman's momentum equation.

2 PROBLEM FORMULATION

Consider a cylindrical microcapillary packed with charged spherical microparticles of diameter, d_p, as illustrated in Fig. 1. The zeta potential at the surface of the solid phase is ζ_p. The liquid through the porous structure is assumed to be an incompressible, Newtonian, symmetric monovalence electrolyte of density, ρ, and viscosity, μ. The porous medium is assumed to be homogeneous and the boundary effects are neglected. Two key parameters characterizing a porous medium are porosity and tortuosity. The porosity is defined as $\phi = V_f / V$, where V_f and V are the void and total volumes of the porous medium, respectively. The tortuosity is defined as $\tau = L_e / L$, where L_e is the effective length of travel for flow along the pore path and L is the physical length of the porous structure. The other two associated factors are pore size, $d_{pore}=2R_{pore}=2\phi d_p / 3(1-\phi)$,, and Darcy permeability, K, which are defined in following sections. These structure-related parameters can be determined by experiment. The AC electroosmotic flow in open and closed microcapillary will be discussed.

2.1 Flow in an open-end packed microchannel

In this situation, the flow is sorely electroosmosis-driven and no pressure gradient is present. We use so-called capillary model [6], in which the porous medium is assumed to be equivalent to a series of parallel tortuous tubules with effective pore size, d_{pore}. The liquid velocity field, $u(r, t)$ in the cylindrical tubules is governed by the Navier-Stokes equation [7]

$$\rho \frac{\partial u(r,t)}{\partial t} - \mu \frac{1}{r}\frac{\partial}{\partial r}\left[r \frac{\partial u(r,t)}{\partial r} \right] = E(t)\rho_e(r) \qquad (1)$$

where $\rho_e(r)$ is the local volumetric net charge density of the electrolyte, and is governed by Boltzmann equation

$$\rho_e(r) = -2n_0 e_0 \sinh\left[\frac{e_0\psi(r)}{k_b T}\right] \tag{2}$$

Here $\psi(r)$ is the electrostatic potential of the *EDL*, and it is solved to follow an analytical scheme developed in ref. [2]. e_0 is the elementary charge, n_0 is the ionic concentration in the bulk liquid phase (i.e., far from the charged surfaces), k_b is the Boltzmann constant, T is the absolute temperature.

Introducing the following dimensionless parameters:

$$\bar{u} = \frac{u}{u_s} \quad \bar{t} = \frac{t}{t_{diff}} \quad \bar{r} = \frac{r}{R_{pore}} \quad \Psi = \frac{e_0\psi}{k_b T} \quad u_s = -\frac{\varepsilon_r\varepsilon_0}{\mu}E_0\zeta_p \tag{3}$$

We can nondimensionlize Eq. (1) as

$$\frac{\partial\bar{u}}{\partial\bar{t}} - \frac{1}{\bar{r}}\frac{\partial}{\partial\bar{r}}\left(\bar{r}\frac{\partial\bar{u}}{\partial\bar{r}}\right) = \frac{(\kappa R_{pore})^2}{\Psi_s E_0}\sinh\left[\Psi(\bar{r})\right]E(\bar{t}) \tag{4}$$

where the reference time $t_{diff}=\rho R^2_{pore}/\mu$ is the viscous diffusion time scale. $\psi_s=e_0\zeta_p / k_bT$. κ is the Debye-Hückel parameter, defined as $\kappa=(2n_0e_0^2/\varepsilon_r\varepsilon_0k_bT)^{1/2}$. ε_r is the dielectric constant of the electrolyte and ε_0 is the permittivity of vacuum. Eq. (4) is subject to the initial and boundary conditions

$$\bar{t} = 0 \quad \bar{u} = 0 \tag{5a}$$

$$\bar{r} = 0 \quad \frac{\partial\bar{u}}{\partial\bar{r}} = 0 \quad \bar{r} = 1 \quad \bar{u} = 0 \tag{5b}$$

Using the Green's function method, we can obtain an exact solution to Eq. (4) as

$$\bar{u}(\bar{r},\bar{t}) = \int_{\tau=0}^{\bar{t}}\int_{\xi=0}^{1} G(\bar{r},\bar{t}\,|\,\xi,\tau)\left\{\frac{(\kappa R_{pore})^2}{\Psi_s E_0}\sinh\left[\Psi(\xi)\right]E(\tau)\right\}d\xi d\tau \tag{6}$$

where $G(\bar{x},\bar{t};\xi,\tau)$ is the Green's function expressed as [2]

$$\begin{aligned} &G(\bar{r},\bar{t}\,|\,\xi,\tau) \\ &= H(\bar{t}-\tau)\sum_{n=1}^{\infty}\frac{2J_0(\lambda_n\bar{r})}{J_1^2(\lambda_n)}\xi J_0(\lambda_n\xi)\exp[-\lambda_n^2(\bar{t}-\tau)] \end{aligned} \tag{7}$$

Here λ_n are the positive roots of the zero-order Bessel function $J_0(\lambda_n)=0$, and $H(t-\tau)$ is the Heaviside step function.

Considering the application of a sinusoidally alternating electric field with an angle frequency ω, $E(t) = E_0 e^{i\omega t}$, we can show that Eq. (6) can be expressed as

$$\begin{aligned} \bar{u}(\bar{r},\bar{t}) &= REAL\left[\frac{2(\kappa R_{pore})^2}{\Psi_s}\sum_{n=1}^{\infty}C_n\frac{J_0(\lambda_n\bar{r})}{J_1^2(\lambda_n)}\frac{\exp(i\beta^2\bar{t})-\exp(-\lambda_n^2\bar{t})}{\lambda_n^2+i\beta^2}\right] \\ &= \frac{2(\kappa R_{pore})^2}{\Psi_s}\sum_{n=1}^{\infty}C_n\frac{J_0(\lambda_n\bar{r})}{J_1^2(\lambda_n)}\frac{\lambda_n^2\cos(\beta^2\bar{t})+\beta^2\sin(\beta^2\bar{t})-\lambda_n^2\exp(-\lambda_n^2\bar{t})}{\lambda_n^4+\beta^4} \end{aligned} \tag{8}$$

where $C_n = \int_{\xi=0}^{1}\xi J_0(\lambda_n\xi)\sinh\left[\Psi(\xi)\right]d\xi$. "*REAL*" denotes the real part of the solution. i is the unit imaginary number. β is defined as $\beta = R_{pore}/\delta_s$, representing the aspect ratio of the tubule radius R_{pore} to the Stokes penetration depth δ_s, defined as $\delta_s = \sqrt{\mu/(2\pi\rho f)}$. (here $f=\omega/2\pi$ is the frequency of the applied electric field).

Integrating Eq. (8) along the radius of the cylindrical tubule gives the mean velocity,

$$\begin{aligned} \bar{u}_m(\bar{t}) &= 2\int_{\bar{r}=0}^{1}\bar{r}\,\bar{u}(\bar{r},\bar{t})d\bar{r} \\ &= \frac{4(\kappa R_{pore})^2}{\Psi_s}\sum_{n=1}^{\infty}C_n\frac{1}{\lambda_n J_1(\lambda_n)}\frac{\lambda_n^2\cos(\beta^2\bar{t})+\beta^2\sin(\beta^2\bar{t})-\lambda_n^2\exp(-\lambda_n^2\bar{t})}{\lambda_n^4+\beta^4} \end{aligned} \tag{9}$$

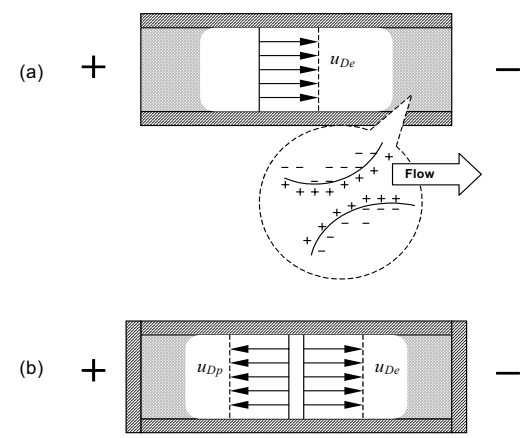

Fig. 1. Schematic illustrations of the AC electroosmosis in porous media. (a) flow in the packed microcapillary connected with two reservoirs. (b) flow in the packed microcapillary with two closed ends. Where u_{De} is the filter (Darcy) velocity due to electroosmosis, and u_{Dp} is the filter (Darcy) velocity due to backpressure.

Under the volume averaging method, the macroscopic filter velocity (Darcy velocity) of the fluid due to EO can be expressed as the mean velocity in each tubule taking into account of the tortuosity τ and the porosity ϕ, as

$$\begin{aligned} \bar{u}_{De}(\bar{t}) &= \frac{\phi}{\tau}\bar{u}_m(\bar{t}) \\ &= \frac{\phi}{\tau}\frac{4(\kappa R_{pore})^2}{\Psi_s}\sum_{n=1}^{\infty}\frac{C_n}{\lambda_n J_1(\lambda_n)}\frac{\lambda_n^2\cos(\beta^2\bar{t})+\beta^2\sin(\beta^2\bar{t})-\lambda_n^2\exp(-\lambda_n^2\bar{t})}{\lambda_n^4+\beta^4} \end{aligned} \tag{10}$$

From Eq. (10) we can further show the expression of the frequency-dependent maximum Darcy velocity as

$$\left|\bar{u}_{De}\right|_{\max}(f)=\frac{\phi}{\tau}\frac{4(\kappa R_{pore})^2}{\Psi_s}\sum_{n=1}^{\infty}\frac{C_n}{\lambda_n J_1(\lambda_n)}\frac{1}{\sqrt{\lambda_n^4+\beta^4}} \tag{11}$$

2.2 Flow in a closed-end packed microchannel

In a microcapillary with closed ends, the electroosmotic flow induces a backpressure gradient. The backpressure gradient in turn generates a counter-flow to balance the electroosmotic volume flow, resulting in a zero flow rate. In porous media, no matter the flow is pressure-driven or electroosmosis-driven, the fluid velocity is represented by a uniform filter (Darcy) velocity u_D. Thus to balance the volumetric electroosmosis-driven flow, the back flow velocity, u_{Dp}, which is driven by the backpressure, must equal in magnitude to the flow velocity, u_{De} driven by electroosmosis (illustrated in Fig. 1(b)), i.e.,

$$\bar{u}_{Dp}(\bar{t})=\bar{u}_{De}(\bar{t}) \tag{12}$$

Using the Brinkman's momentum equation for general pressure-driven flow in porous media, and neglecting the inertial forces and the boundary effect, we have

$$\frac{\rho}{\phi}\frac{du_{Dp}(t)}{dt}=-\frac{\partial p(t)}{\partial z}-\frac{\mu}{K}u_{Dp}(t) \tag{13}$$

Here $u_{Dp}(t)$ is the pressure-driven Darcy velocity through the porous medium inside the microcapillary. Where the Darcy permeability K is defined by the *Carman-Kozeny* equation [6], $K=\phi^3 d_p^2/a(1-\phi)^2$, with $a=150$ being the Ergun constant [8]. The non-dimensionlized form of Eq. (13), using the reference pressure p_0 and length L, is

$$\frac{\partial\bar{p}(\bar{t})}{\partial\bar{z}}=-\frac{L}{p_0}\frac{\mu}{K}u_s\left[\bar{u}_{Dp}(\bar{t})+\frac{K}{\phi R_{pore}^2}\frac{d\bar{u}_{Dp}(\bar{t})}{d\bar{t}}\right] \tag{14}$$

Substitute Eq. (12) into Eq. (14), we obtain the expression for the periodically oscillating pressure gradient

$$\frac{\partial\bar{p}(\bar{t})}{\partial\bar{z}}=-\frac{L}{p_0}\frac{\phi}{\tau}\frac{\mu}{K}u_s\frac{4(\kappa R_{pore})^2}{\Psi_s}\sum_{n=1}^{\infty}\frac{C_n}{\lambda_n J_1(\lambda_n)}\frac{\left(\lambda_n^2+\frac{K\rho\omega}{\mu\phi}\beta^2\right)\cos(\beta^2\bar{t})+\left(\beta^2-\frac{K\rho\omega}{\mu\phi}\lambda_n^2\right)\sin(\beta^2\bar{t})}{\lambda_n^4+\beta^4} \tag{15}$$

From Eq. (15), we obtain frequency-dependent maximum pressure gradient as

$$\left|\frac{\partial\bar{p}}{\partial\bar{z}}\right|_{\max}(f)=-\frac{L}{p_0}\frac{\phi}{\tau}\frac{\mu}{K}u_s\frac{4(\kappa R_{pore})^2}{\Psi_s}\sum_{n=1}^{\infty}\frac{C_n}{\lambda_n J_1(\lambda_n)}\frac{\sqrt{1+\left(\frac{K\rho\omega}{\mu\phi}\right)^2}}{\sqrt{\lambda_n^4+\beta^4}} \tag{16}$$

3 RESULTS AND DISCUSSION

In the parametric study, the calculations are based on the values reported by Zeng *et al* [4]. The properties of the working solution were reported as: ionic strength 7.5 μM, zeta potential –95 mV, porosity 0.37, and tortuosity 1.5.

Several important parameters are also highlighted before discussion. The characteristic viscous diffusion time scale is denoted by the reference time $t_{diff}=\rho R^2_{pore}/\mu$. The time period for excitation electric field is denoted by $t_E=1/f$. From the exponential term in Eq. (10), we can further estimate the characteristic time scale for the AC electroosmotic flow to reach its time-periodic steady state by choosing $\lambda_1^2\mu t^*/\rho R^2_{pore}=1$. Then $t^*=\rho R^2_{pore}/\mu\lambda_1^2$, where $\lambda_1=2.405$ determined form $J_0(\lambda_n)=0$. The corresponding intrinsic frequency of the system is defined as $f^*=1/t^*=\mu\lambda_1^2/\rho R^2_{pore}$. And we can infer that β represents the square root of the aspect ratio of the diffusion time scale to the period of electric field, i.e., $\beta=(2\pi\, t_{diff}/\, t_E)^{1/2}$.

3.1 Oscillating flow velocity in an open-end packed microchannel

The steadily time-periodic AC electroosmotic flow velocity for two-cycle periods in a packed microchannel with open ends are shown in Fig. 2. It is clearly shown that the flow presents a harmonic sinusoidal oscillation only with different magnitudes and phase lags. Fig. 2 gives a comparison of the effects of three different excitation frequencies for a fixed pore size. It is obvious that, for the same packing condition, using AC voltage of higher frequency decreases the EOF velocity. This scenario can be anticipated because under much high frequency, the electric field changes its direction so fast that the flow can never get developed across the bulk intraparticle domain. In case of very high frequency, corresponding to a large value of β, the diffusion time scale is much greater than the oscillation time period, i.e., $t_{diff} > t_E$. Therefore there is no sufficient time for the flow momentum to diffuse far into the intraparticle bulk phase. Thus the perturbed area is restricted only in a thin layer near the particle surface, while the fluid in the bulk phase remains stationary. This typical length scale of the oscillatory laminar viscous flow in response to a harmonic external excitation is represented by the frequency-dependent Stokes penetration depth, δ_s. Furthermore, the flow lags behind the excitation field with larger phase lag for higher frequency.

For a better understanding of the frequency-dependent velocity, we compare the magnitude of the oscillating velocity versus complete domain of frequency shown in Fig. 3, for three cases of different pore sizes. In accord with above analysis, for a fixed pore size, the magnitude of maximum velocity decreases with increasing excitation frequency. With increasing pore size, the magnitude of the maximum velocity gets higher in case of low frequency domain (lower than about 0.02f^*), and gets lower in case of high frequency domain (higher than about 0.2 f^*).

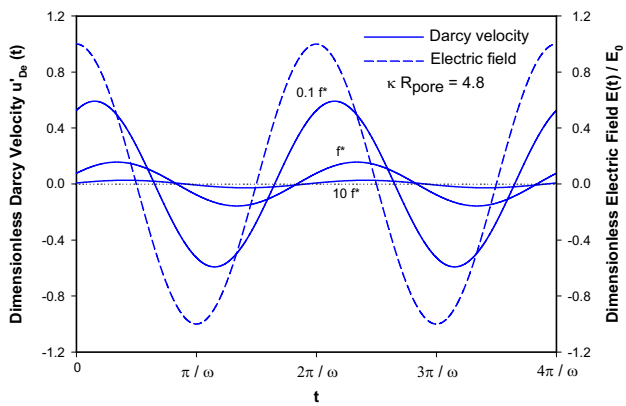

Fig. 2. Dimensionless time-periodic oscillating Darcy electroosmotic flow velocity versus time for three different excitation frequencies at a fixed pore size.

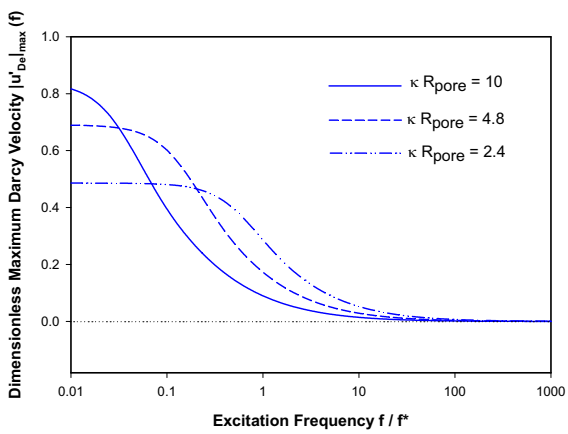

Fig. 3. Dimensionless maximum Darcy electroosmotic flow velocity versus excitation frequency, for three different pore sizes.

3.2 Oscillating backpressure in a closed-end packed microchannel

Fig. 4 presents the steadily time-periodic oscillation of the backpressure in a capillary of closed ends. It is shown that the backpressure associated with the counter-flow to balance the AC electroosmotic flow after application of the alternating voltage also presents a harmonic oscillation.

The magnitude of the maximum pressure drop versus the excitation frequency domain is shown in Fig. 5, for case study of three pore sizes. The maximum pressure drop generated by small pore size (corresponding to a smaller packing particle size) is always greater than that generated by large pore size (corresponding to a large packing particle size), for the entire domain of the excitation frequency. This result is in agreement with the experimental observations by Paul *et al* [3] who reported that the pressure generated per applied DC volt increases with smaller diameters of packing beads. It is also apparent in Fig. 5 that, for a fixed pore size, the backpressure decreases with increasing excitation frequency, until it reaches its system intrinsic frequency *f**, and from which the backpressure increases with increasing excitation frequency.

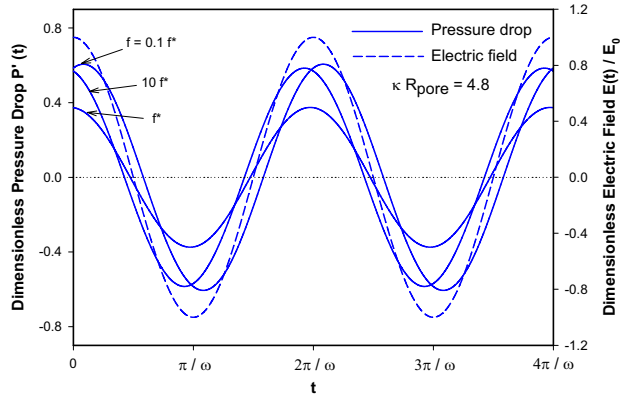

Fig. 4. Dimensionless time-periodic oscillating backpressure drop versus time for three different excitation frequencies at a fixed pore size.

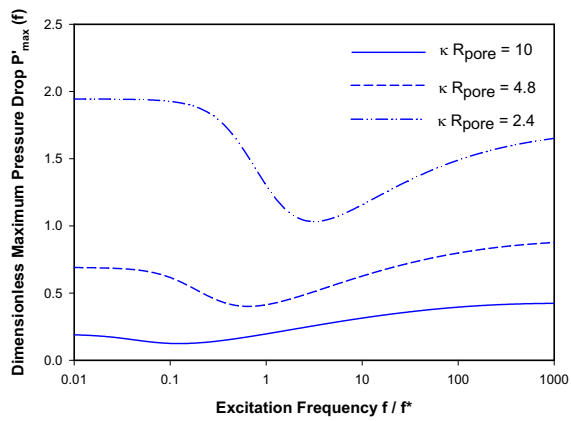

Fig. 5. Dimensionless maximum backpressure drop versus excitation frequency for three different pore sizes.

REFERENCES

[1] P. Dutta and A. Beskok, Anal. Chem. 73, 5097, 2001.

[2] Y.J. Kang, C. Yang, and X.Y. Huang, Int. J. Eng. Sci. 40, 2203, 2002.

[3] P. H. Paul, D. W. Arnold, and D. J. Rakestraw, in: Proceedings of the Micro Total Analysis Systems '98 Workshop, Banff, Canada, 1998.

[4] S. Zeng, C. H. Chen, J. C. Jr Mikkelsen, and J. G. Santiago, Sensors and Actuators B, 79, 107, 2001.

[5] H. Nakagawa, M. Sato, S. Kitagawa, and T. Tsuda, Anal. Chem. 75, 3180, 2003.

[6] M. Kaviany, "Principles of Heat Transfer in Porous Media," Springer-Verlag, New York., 1995.

[7] R. F. Probstein, "Physicochemical Hydrodynamic," John Wiley & Sons, New York., 1994.

[8] C. T. Hsu, and P. Cheng, Int. J. Heat Mass Transfer 33, 1587, 1990.